

Spectroscopic ellipsometric analysis of interfaces: Comparison of alloy and effective-medium-approximation approaches to a CdMgTe multilayer system

T. H. Ghong, T. J. Kim, and Y. D. Kim^{a)}

Department of Physics and Research Institute for Information Display, Kyung Hee University, Seoul 130-701, Korea

D. E. Aspnes

Department of Physics, North Carolina State University, North Carolina

(Received 15 April 2004; accepted 8 June 2004)

We discuss the accuracy and detectability of interface layers in the analysis of ellipsometric spectra in the $\text{Cd}_x\text{Mg}_{1-x}\text{Te}$ system. Using parametric-alloy and effective-medium-approximation (EMA) representations to simulate interfaces in a single-quantum-well structure, we show that EMA analysis overestimates thicknesses of alloy interfaces by more than a factor of 3. While detailed results will clearly depend on the nature of the epitaxial materials involved, the results suggest that analyses of interfaces by the EMA should be done with caution. © 2004 American Institute of Physics. [DOI: 10.1063/1.1779965]

It is well known that interfaces and rough surfaces can be represented as mixtures of adjacent materials. In optical analysis, the dielectric functions of these layers are generally expressed using the effective-medium approximation (EMA),^{1,2} which is valid for physical mixtures, i.e., either in the absence of alloying on the atomic scale, or in situations where changes of the dielectric response with composition are not significant. Examples of the latter situation include interfaces involving elemental, binary, or amorphous materials with oxides or rough surfaces. As a result of its simplicity and the fact that it works quite well for a wide range of systems, the EMA together with multilayer models has been widely used to characterize grown films,^{3,4} investigate surface roughness,⁵ and monitor the growth of the films^{6,7} by spectroscopic ellipsometry (SE).

However, the assumption of physical rather than atomic mixing of adjacent constituents is not expected to be valid in all cases. The EMA is appropriate where each “grain” of material is assumed to be large enough to retain its own characteristic bulk dielectric function, but small compared to the optical wavelengths involved in the measurement. The EMA effectively averages the two spectra, taking into account the electric polarization that occurs at the boundaries.¹ Since most multilayer structures used in current thin-film technology are grown epitaxially, it may be more realistic to represent interfaces as 50% alloys of the adjacent materials⁸ rather than the EMA. This should be particularly true for materials, such as crystalline semiconductors, which exhibit pronounced energy-dependent structure in their optical spectra.

In this work, we examine the effects of considering interfaces as either EMA or alloy mixtures, with particular emphasis on analyses of alloy interfaces by the EMA. We specifically consider $\text{Cd}_{1-x}\text{Mg}_x\text{Te}$ alloys and related heterostructures, which have attracted much attention for optoelectronic devices because their band gaps cover the entire visible range and their lattice mismatches with bulk MgTe or

CdTe can be as small as 1.0%. Even though the properties of the binary endpoint CdTe is well known,^{9,10} only a few studies of the critical point energies of CdMgTe alloys have been reported so far.^{11,12} For the alloy calculations, we fill the gaps in data by using the parametric model¹³ to interpolate between existing $\text{Cd}_{1-x}\text{Mg}_x\text{Te}$ spectra, which have been reported from 1.5 to 6.0 eV for compositions x of 0.00, 0.23, 0.31, and 0.43. These data were obtained on films grown epitaxially on [001] GaAs substrates by molecular-beam epitaxy. This approach allows analytic representations of the alloy dielectric functions to be obtained for any intermediate value of x .¹⁴

Data for $\text{Cd}_{1-x}\text{Mg}_x\text{Te}$ alloys with $x=0.00$, 0.23, 0.31, and 0.43 are shown in Fig. 1 as the solid lines.¹² Only the imaginary part ϵ_2 of the complex dielectric function $\epsilon=\epsilon_1+i\epsilon_2$ is shown for simplicity, even though all analyses reported here were done on both ϵ_1 and ϵ_2 simultaneously.

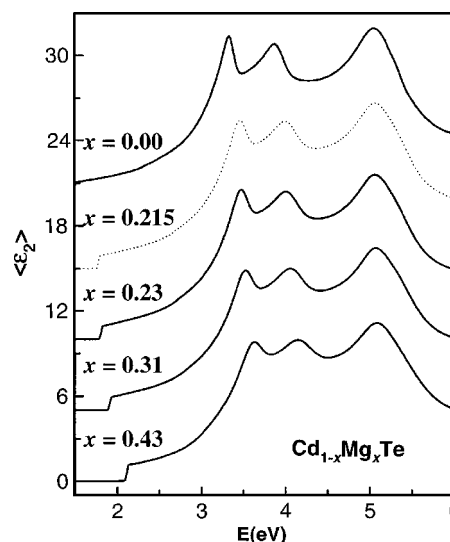


FIG. 1. Solid lines: Data for the imaginary parts of $\langle\epsilon\rangle$ for $\text{Cd}_{1-x}\text{Mg}_x\text{Te}$ alloys with $x=0.0$, 0.23, 0.31, and 0.43 (from Ref. 12). Dotted line: Alloy spectrum for $x=0.215$ calculated in the parametric representation.

^{a)}Electronic mail: ydkim@oprl.khu.ac.kr

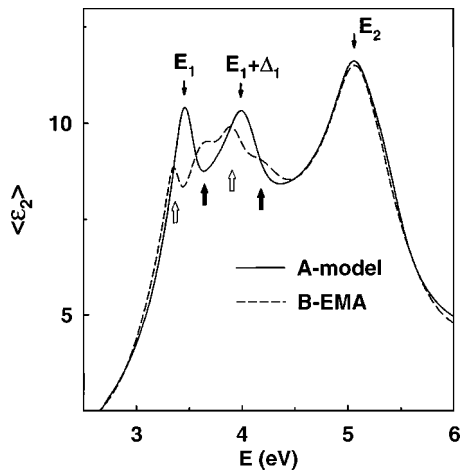


FIG. 2. Comparison of $\text{Cd}_{0.785}\text{Mg}_{0.215}\text{Te}$ spectra calculated by assuming mixing on the atomic (alloy, solid line) and physical (dashed line) scales.

Also shown as an example is a $x=0.215$ spectrum calculated in the parametric model, which represents 50% alloying of the $x=0.00$ and 0.43 materials. Our detailed procedure for calculating this spectrum is described in Ref. 14.

In Fig. 2, we contrast the good agreement between the calculated alloy spectrum for $x=0.215$ and the $x=0.23$ data seen in Fig. 1 with the EMA result. The basic EMA equation is

$$\frac{\epsilon - \epsilon_h}{\epsilon + 2\epsilon_h} = f_a \frac{\epsilon_a - \epsilon_h}{\epsilon_a + 2\epsilon_h} + f_b \frac{\epsilon_b - \epsilon_h}{\epsilon_b + 2\epsilon_h}, \quad (1)$$

where ϵ is the dielectric function of the mixture, ϵ_a and ϵ_b are those of adjacent materials a and b , and ϵ_h is that of the host medium. The Bruggeman EMS is obtained by making the mean-field approximation $\epsilon = \epsilon_h$, which is appropriate for most situations and particularly where the volume fractions f_a and f_b of materials a and b are comparable, as is the case here. We form the EMA spectrum for $x=0.215$ as a 1:1 mixture of the data of Fig. 1 for $x=0$ and $x=0.43$. The result is shown as the dashed curve in Fig. 2. While the overall spectral responses are similar, the physical mixture not surprisingly exhibits characteristics of both CdTe and $\text{Cd}_{0.57}\text{Mg}_{0.43}\text{Te}$, in particular the E_1 and $E_1 + \Delta_1$ critical point structures of both materials. This leads to an unphysical four-peak spectrum in the E_1 and $E_1 + \Delta_1$ region, where the peaks are highlighted by the up arrows, open for CdTe and closed for $\text{Cd}_{0.57}\text{Mg}_{0.43}\text{Te}$. In contrast, that calculated with the parametric model exhibits only two peaks, as it should. These are

$\text{Cd}_{1-x}\text{Mg}_x\text{Te}$ ($x=0.43$)	100 Å
interface	30 Å
CdTe ($x=0.0$)	100 Å
interface	30 Å
$\text{Cd}_{1-x}\text{Mg}_x\text{Te}$ ($x=0.43$)	100 Å
CdTe ($x=0.0$) substrate	

FIG. 3. The single QW structure examined here.

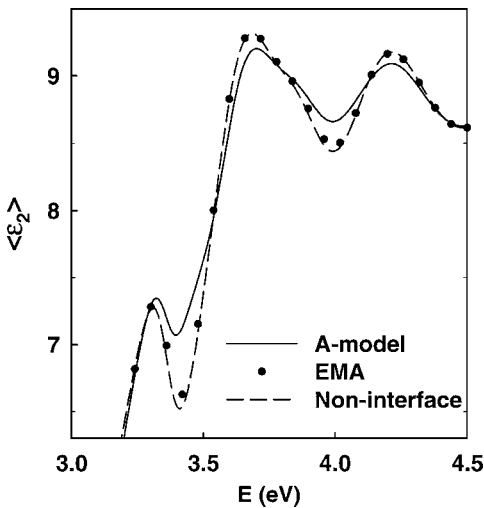


FIG. 4. $\langle \epsilon \rangle$ spectra of the structure of Fig. 3 calculated assuming alloy (solid line), physically mixed (dotted line), and no (dashed line) interfaces. In all cases, the overall thickness is the same.

highlighted by the down arrows. While the overall similarity in line shapes will give qualitatively similar results in optical modeling, it is clear from Fig. 2 that the parametric model would give the best results.

We examine the capabilities of the two representations by applying these results to the analysis of the simple single-quantum-well (QW) structure shown in Fig. 3. We assumed 30 Å thick interfaces of $\text{Cd}_{0.785}\text{Mg}_{0.215}\text{Te}$ on either side of a

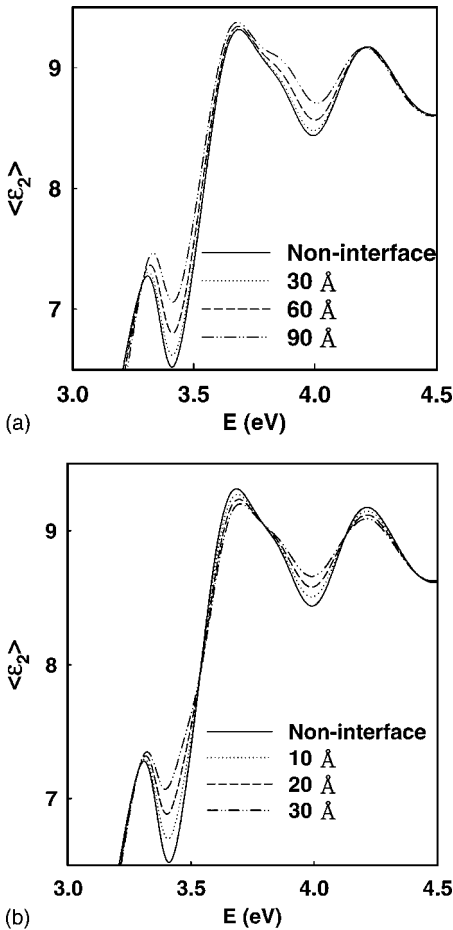


FIG. 5. Changes in $\langle \epsilon \rangle$ with thickness for (a) alloy and (b) EMA interfaces for the structure of Fig. 3.

CdTe QW, with all three layers confined by a $\text{Cd}_{0.57}\text{Mg}_{0.43}\text{Te}$ alloy. The entire structure is assumed to be fabricated on a CdTe substrate. We next use a multilayer model¹⁵ to calculate the pseudodielectric function spectra $\langle\epsilon\rangle$ of the QW system as measured by SE for three cases: The first and second with the interface described by the alloy and Bruggeman EMA models, respectively, and the third with no interface layers but with the original 30 Å thicknesses allocated equally between the QW and the adjacent confining layers, which are now 130 and 115 Å thick, respectively. The results are shown in Fig. 4, with the alloy, EMA, and no-interface calculations shown as the solid, dotted, and dashed lines, respectively. The EMA and no-interface spectra are almost identical, showing that SE would have difficulty detecting the presence of a physically mixed interface. However, the $\langle\epsilon\rangle$ spectrum for the alloyed interfaces is significantly different. While this result does not prove that the current high-quality interfaces produced in current thin-film technology are alloys, it does raise doubts about conclusions obtained about these interfaces on the basis of EMA modeling alone.

To investigate detectability limits, we performed additional calculations reducing the interface thicknesses while keeping the overall thickness constant. The results are shown in Fig. 5(a) for the alloy approach and Fig. 5(b) for the EMA. Figure 5(a) shows significant differences for interfaces only 10 Å wide, whereas the EMA requires over three times more interface material to qualitatively achieve the same amount of change. Thus, in application to the present structure, the EMA would overestimate the thickness of an alloy interface by more than a factor of 3. Even aside from sensitivity issues, this is a significant error. While details may depend on

the natures of the materials and structures being investigated, the present results indicate that interface analysis in epitaxial semiconductor structures using the EMA may not be accurate and in any case should be used with caution.

This work was supported by Grant No. R02-2003-000-10074-0 of the Korea Science and Engineering Foundation and also by the Quantum Photonic Science Research Center at Hanyang University. The work at North Carolina State University was supported by the Office of Naval Research.

¹D. E. Aspnes, *Thin Solid Films* **89**, 249 (1982) and references therein.

²J. L. Freeouf, *Appl. Phys. Lett.* **53**, 2426 (1988).

³Y. Cong, R. W. Collins, G. F. Epps, and H. Windischmann, *Appl. Phys. Lett.* **58**, 819 (1991).

⁴E. C. Paloura, S. Logothetidis, S. Boultafakis, and S. Ves, *Appl. Phys. Lett.* **59**, 280 (1991).

⁵D. E. Aspnes, J. B. Theeten, and F. Hottier, *Phys. Rev. B* **20**, 3292 (1979).

⁶S. Kumar and B. Drevillon, *J. Appl. Phys.* **65**, 3023 (1989).

⁷I. An, H. V. Nguyen, N. V. Nguyen, and R. W. Collins, *Phys. Rev. Lett.* **65**, 2274 (1990).

⁸T. J. Kim, T. H. Ghong, and Y. D. Kim, *J. Korean Phys. Soc.* (to be published).

⁹S. Adachi, T. Kimura, and N. Suzuki, *J. Appl. Phys.* **74**, 3435 (1993).

¹⁰P. Lautenschlager, S. Logothetidis, L. Vina, and M. Cardona, *Phys. Rev. B* **32**, 3811 (1985).

¹¹M. Luttmann, F. Bertin, and A. Chabil, *J. Appl. Phys.* **78**, 3387 (1995).

¹²Y. S. Ihn, T. J. Kim, Y. D. Kim, D. E. Aspnes, and J. Kossut, *Appl. Phys. Lett.* **84**, 693 (2004).

¹³B. Johs, C. M. Herzinger, J. H. Dinan, A. Cornfeld, and J. D. Benson, *Thin Solid Films* **313**, 137 (1998).

¹⁴Y. S. Ihn, T. J. Kim, T. H. Ghong, Y. D. Kim, D. E. Aspnes, and J. Kossut, *Thin Solid Films* **455–456**, 222 (2004).

¹⁵R. M. Azzam and N. M. Bashara, *Ellipsometry and Polarized Light* (North-Holland, Amsterdam, 1977), p. 273.